PHYSICAL REVIEW A VOLUME 43, NUMBER 5 1 MARCH 1991

Helium photoionization between the $N=2$ and $N=3$ thresholds including angular distribution and resonance properties: A K-matrix L^2 basis-set calculation

R. Moccia*
Dipartimento di Chimica e Chimica Industriale, Università di Pisa, Via Risorgimento 35, I-56126 Pisa, Italy

P. Spizzo*
Istituto di Chimica Quantistica ed Energetica Molecolare del Consiglio Nazionale delle Ricerche, Via Risorgimento 35, I-56126 Pisa, Italy

(Received 15 February 1990; revised manuscript received 31 May 1990)

A K-matrix method employing L^2 basis sets has been utilized to investigate the $^1P^\circ$ continuum of helium between the $N=2$ and $N=3$ thresholds (65.4–73.0 eV). The results include the partial and total photoionization cross sections, the asymmetry parameters β, and the positions and the widths of the autoionizing states. Good agreement is found with the available experimental data for the $N=2$ cross section. In agreement with other recent theoretical calculations, at 68.88 eV the total cross section is predicted to be slightly greater than the recommended value that is generally employed to normalize the experimental data.

I. INTRODUCTION

There is a growing interest in photoionization processes at energies where more open channels have the same global symmetry; a feature generally associated with the occurrence of multiply excited autoionizing states. The theoretical study of these processes requires the description of several interacting degenerate continua which, especially in the presence of autoionizing states, is a challenging task. This problem has been generally treated by close-coupling or related methods, which require the solution of a large system of coupled differential equations. Therefore these methods become very cumbersome when many configurations are required for describing accurately the electron correlation or when the system does not have atomic symmetry. Energy-variational methods employing L^2 basis sets, on the other hand, are less affected by these difficulties and their development appears to be a very promising field. In particular, they should allow one to exploit all the experience gained with the electronic structure of molecular systems. Helium provides a reliable test for the capability of the theoretical methods to treat problems of these kinds: highly correlated wave functions are needed to reproduce accurately some fine features of its spectrum, but at the same time no significant discrepancy between theory and experiment may be ascribed to frozen-core or similar approximations. Not surprisingly, therefore, the spectrum of helium between the $N=2$ and $N=3$ thresholds (65.4–73.0 eV) has been the object of extensive experimental[1–16] and theoretical[17–36] study in recent years.

For helium, the spin-orbit effects may be safely neglected, so that the LS coupling is quite adequate and the $^1P^\circ$ continuum is the only one relevant for the ground-state photoionization. Between the above-mentioned thresholds, for each M_L this continuum is fourfold degenerate, corresponding to the asymptotic configurations $1s\epsilon p$ [i.e., $He^+(1s)$ and a p wave of energy ϵ], $2s\epsilon p$, $2p\epsilon s$, and $2p\epsilon d$. Above 69 eV, this continuum is also highly structured, due to the presence of five series of resonances, which, in the independent-electron limit, correlate to configurations of the forms $3snp$, $3pns$, $3pnd$, $3dnp$, and $3dnf$. The classification of these autoionizing states has raised considerable interest and several schemes have been proposed.[32] This work employs the notation proposed by Herrick and Sinanoglu,[20] as refined by Lin,[32] which appears to be the best known and most largely employed. In this scheme, the resonances between the $N=2$ and $N=3$ thresholds are conveniently labeled as K_n, where $K=-2,-1,0,1,2$ is related to the Runge-Lenz vector (an approximate constant of the motion) while n is an outer quantum number which starts from 3 for $|K|=1$ and from 4 for $|K|\neq 1$. For conciseness, we have dropped in the text the further labels N, T, and A, since $N=3$ for all these states, while T and A are redundant when the global symmetry is specified. The label A (which, for the reader's convenience, has been kept in the tables) is related to the autoionizing widths, which are large for $A=1$ (series with $K=\pm 1$), small for $A=-1$ ($K=0,2$), and very small for $A=0$ ($K=-2$). The $K=1$ series is easily seen in the photoionization from the ground state while only the lowest term of the $K=-1$ series has been observed.[8,16] The other series are almost forbidden to autoionize and their experimental detection in photoionization from the ground state appears improbable in the near future, with the possible exception of the 2_4 resonance.

In previous work,[37–42] an efficient L^2 technique has been developed to treat accurately single-channel problems also in the presence of narrow resonances. In the present work, this technique will be extended to treat many-channel problems through a K-matrix method.[43] Unless otherwise stated, all quantities are expressed in atomic units.

II. METHOD OF CALCULATION

The method employed in the present work is based upon the energy-variational approach, originally pioneered by Fano,[43] which may be adapted to the usual L^2 approach of quantum chemistry. No orthogonality conditions will be invoked, since the aim is to realize the fastest convergence with the basis-set size. The method, similarly to the close coupling employed for atoms, is essentially a configuration interaction (CI) carried out with a basis set including localized correlating functions and (formally) the asymptotic continua of the relevant channels. By a judicious choice of these basis sets, the resulting secular equation is solved, at a given energy E lying in the continuum, by the reaction K-matrix technique, which yields the coupled integral equations (3) for the half-off-shell K-matrix elements. This integral equation is solved by introducing a discrete quadrature upon the grid points supplied by a discretized representation of the "unperturbed" states, which turns the integral equation into a linear system. The matrix elements at arbitrary values of the continuous energy indices are interpolated upon the grid points. The implementation of the method, although straightforward in principle, requires a careful consideration of several details, which are explained in Secs. II C and II D.

A. Choice of the bases

To have a definite notation, let us consider an atomic system and assume the validity of the LS coupling. The L, S, M_L, and M_S labels of the total system may be considered specified once for all and will be dropped in the following.

The formal variational basis set is composed of $N+1$ subspaces, which are numbered from 0 to N and indexed with Greek letters. The zeroth subspace is spanned by localized functions, which are needed to reproduce accurately the bound and autoionizing states and to take into account the short-range electron correlation in the continuum states. The subspaces numbered from 1 to N will be called partial wave channel (PWC) subspaces; in this case the subspace index specifies the level $I=N_I L_I S_I$ of the residual ion and the angular momentum l of the outer electron; note that several PWC's may correspond to the same ionic level. These subspaces are spanned by spin- and symmetry-adapted antisymmetrized products of a given ion state $|\Phi^+_{IM_LM_S}\rangle=|\Phi^+_{N_IL_IS_IM_LM_S}\rangle$ and a partial wave. The $|\Phi^+_{IM_LM_S}\rangle$ may be exact or approximate bound states of the residual ion with energy E_I^+, which are assumed to be orthonormal and to diagonalize the Hamiltonian of the ion. These N PWC subspaces are conveniently ordered in increasing ion energy E_I^+: for a given total energy E, those with $E_I^+<E$ (say the first n) will be called open PWC's and the remaining ones closed PWC's. In the following, a subspace index α or γ designates explicitly an open PWC subspace (1 to n), while an index β denotes an arbitrary subspace (0 to N).

Let $\hat{Q}_\beta$ be the projector onto the βth subspace, $\hat{Q}_\beta\hat{H}\hat{Q}_\beta$ the restriction of the Hamiltonian to this subspace, and $|\Phi_{\beta E}\rangle$ its eigenfunctions

$$\hat{Q}_\beta\hat{H}\hat{Q}_\beta|\Phi_{\beta E}\rangle=E|\Phi_{\beta E}\rangle$$

which will be the formal basis set for the K-matrix calculations. For ease of writing, the same notation has been employed for discrete and continuous eigenfunctions, normalized to unity and $\delta(E-E')$, respectively.

Note that in the PWC subspaces ($\beta>0$) the eigenfunctions of $\hat{Q}_\beta\hat{H}\hat{Q}_\beta$ have the form

$$|\Phi_{\beta E}\rangle=\hat{Q}|\Phi^+_{IM_LM_S}\psi_{\epsilon lmm_s}\rangle,\quad E=E_I^+ +\epsilon$$

where $|\psi_{\epsilon lmm_s}\rangle$ are bound ($\epsilon<0$) or unbound ($\epsilon\geq 0$) one-electron functions and $\hat{Q}$ is a projector for the global symmetry. The PWC eigenfunctions may be chosen real (at least for $M_L=0$) and their $|\psi_{\epsilon lmm_s}\rangle$ behave asymptotically as standing waves.

Clearly, inside each subspace the $|\Phi_{\beta E}\rangle$ are orthogonal and diagonalize the total Hamiltonian, but overlap and Hamiltonian matrix elements between different subspaces will in general be nonzero, and thus the corresponding projectors $\hat{Q}_\beta$ are not required to satisfy $\hat{Q}_\beta\hat{Q}_{\beta'}=\delta_{\beta\beta'}\hat{Q}_\beta$. Also, no strong-orthogonality constraints are imposed between the ion states $|\Phi^+_{IM_LM_s}\rangle$ and the waves $|\psi_{\epsilon lmm_s}\rangle$. It should be noted that the ion states $|\Phi^+_{IM_LM_S}\rangle$ may be correlated states of arbitrary type.

In the present approach, the correlation effects on the outer electron are more conveniently taken into account by employing a large zeroth subset rather than considering several closed channels. Indeed, a properly chosen zeroth subset may be considered a resummation of all the open and many closed PWC subspaces, resulting in an accelerated convergence of the variational expansion.

B. The K-matrix method

Corresponding to the n channels which are open at energy E, let us consider n real trial functions of the form

$$|\Psi_{\alpha E}\rangle=|\Phi_{\alpha E}\rangle+\sum_{\beta'}\sum\!\!\!\!\!\!\int dE'|\Phi_{\beta' E'}\rangle\mathrm{P}\frac{1}{E-E'}K_{\beta' E',\alpha E}\quad(1)$$

where P denotes the principal part of the integral and for each subset $\sum\!\!\!\!\!\!\int$ denotes the summation over its discrete part and the integration over the continuous one. The expansion coefficients are determined by imposing

$$\langle\Phi_{\beta' E'}|\hat{H}-E|\Psi_{\alpha E}\rangle=0\quad(2)$$

for all the basis-set functions $|\Phi_{\beta' E'}\rangle$ and this leads to the system of coupled integral equations

$$K_{\beta' E',\alpha E}-\sum_{\beta''\neq\beta'}\sum\!\!\!\!\!\!\int dE''V_{\beta' E',\beta'' E''}(E)\mathrm{P}\frac{1}{E-E''}K_{\beta'' E'',\alpha E}=V_{\beta' E',\alpha E}(E)\quad(3)$$

where

$$V_{\beta' E',\beta'' E''}(E)=\langle\Phi_{\beta' E'}|\hat{H}-E|\Phi_{\beta'' E''}\rangle=H_{\beta' E',\beta'' E''}-ES_{\beta' E',\beta'' E''}\ .$$

It is easy to show that for real energies the K matrix on the energy shell $\mathbf{K}(E)$ defined by $K_{\alpha'\alpha}(E)=K_{\alpha' E,\alpha E}$ is a

real symmetric matrix. The states $|\Psi_{\alpha E}\rangle$ satisfy

$$\langle\Psi_{\alpha' E'}|\Psi_{\alpha E}\rangle=\left[\delta_{\alpha'\alpha}+\pi^2\sum_{\gamma}K_{\gamma E,\alpha' E}K_{\gamma E,\alpha E}\right]\delta(E-E')\ , \tag{4}$$

$$\langle\Psi_{\alpha' E'}|\hat{H}|\Psi_{\alpha E}\rangle=E\left[\delta_{\alpha'\alpha}+\pi^2\sum_{\gamma}K_{\gamma E,\alpha' E}K_{\gamma E,\alpha E}\right]\times\delta(E-E')\ . \tag{5}$$

These relations are not new, but to our knowledge their general validity was established before only for orthogonal projectors $\hat{Q}_\beta\hat{Q}_{\beta'}=\delta_{\beta\beta'}\hat{Q}_\beta$, a restriction which may cause an extreme slowness of convergence in a variational expansion. The proof of Eq. (4) is given in the Appendix; Eq. (5) follows immediately from Eqs. (2) and (4).

Two sets of complex orthonormal eigenfunctions may now be defined by

$$|\Psi_E^{(\pm)}\rangle=\{|\Psi_{1E}^{(\pm)}\rangle\cdots|\Psi_{nE}^{(\pm)}\rangle\}$$
$$=\{|\Psi_{1E}\rangle\cdots|\Psi_{nE}\rangle\}\{[\mathbf{1}\pm i\pi\mathbf{K}(E)]^{-1}\boldsymbol{\Delta}^{(\pm)}(E)\ .$$

The diagonal matrices $\boldsymbol{\Delta}^{(\pm)}(E)$ have elements $\Delta_{\alpha'\alpha}^{(\pm)}(E)=\delta_{\alpha\alpha'}e^{\pm i\xi_{\alpha E}}$, where $\xi_{\alpha E}$ is the total phase shift of $|\Phi_{\alpha E}\rangle$, which includes the Coulomb contribution $\arg\Gamma(l_\alpha+1-iZ/k_{\alpha E})-\pi l_\alpha/2$. The asymptotic expression of $|\Psi_{\alpha E}^{(-)}\rangle$ presents ingoing waves in all the open channels, but an outgoing wave only in the αth channel and with zero phase shift. Therefore these functions satisfy the boundary conditions for the photoionization process, while the states $|\Psi_{\alpha E}^{(+)}\rangle$ are suitable for describing the scattering.[44] The scattering matrix $\mathbf{S}(E)$ is related to $\mathbf{K}(E)$ by[45]

$$\mathbf{S}(E)=\langle\Psi_E^{(-)}|\Psi_E^{(+)}\rangle=\boldsymbol{\Delta}^{(+)}(E)\frac{\mathbf{1}-i\pi\mathbf{K}(E)}{\mathbf{1}+i\pi\mathbf{K}(E)}\boldsymbol{\Delta}^{(+)}(E)\ . \tag{6}$$

Note that all the time-consuming steps involve only real quantities, while the more usual direct determination of the states $|\Psi_{\alpha E}^{(\pm)}\rangle$ requires much heavier calculations with complex quantities.[34,36]

C. The L^2 basis sets for the PWC continua

The spectra of the projected Hamiltonians $\hat{Q}_\beta\hat{H}\hat{Q}_\beta$ have been represented by the L^2 technique developed in previous work,[39–41] which yields satisfactory representations of single-channel continua not only for Hamiltonians like $\hat{Q}_\beta\hat{H}\hat{Q}_\beta$ but also in the presence of strong correlations between the outer electron and the core.

L^2 representations for the four PWC subspaces employed in the present case have been obtained by diagonalizing the Hamiltonian upon bases of spin- and symmetry-adapted Slater determinants of the forms $1snp$, $2snp$, $2pns$, and $2pnd$. Here $1s$, $2s$, and $2p$ are the exact states of He^+ and the orbitals nl employed to represent the electron wave ψ include, besides Slater-type orbitals (STO) and hydrogenic functions, a large number of STO times a cosine (STOC) functions

$$\chi_{\zeta klm}(\mathbf{r})=N_{\zeta kl}r^l e^{-\zeta r}\cos(kr)Y_{lm}(\hat{\mathbf{r}})$$

with the k values equally spaced according to $k_j=(j+\frac{1}{2})\pi/R_0$ so that all these orbitals have a node in R_0, which in this calculation was chosen to be 200. In the present case, where the long-range potential is Coulombic, the diagonalization of $\hat{Q}_\beta\hat{H}\hat{Q}_\beta$ on the above bases yields a set of unit-normalized variational states $|\phi_{\beta j}\rangle$ which includes accurate approximations for its lower bound states, a few wave packets in the higher Rydberg region, many narrow wave packets with closely spaced energies in the continuum (about one for each STOC) and a number of broad wave packets at the upper end of the spectrum.

The $|\phi_{\beta j}\rangle$ referred to as narrow wave packets are very accurate inside a sphere of radius about R_0, i.e., in it they are almost exactly proportional to the continuous $\delta(E)$-normalized eigenstates $|\Phi_{\beta E}\rangle$ of the same energy $E=E_{\beta j}$. If R_0 is large enough, the outer orbital of $|\phi_{\beta j}\rangle$ behaves as a shifted Coulomb wave in a wide region of space. The analysis of its behavior in this region yields its phase shift $\xi_{\beta j}$ and a normalization constant $C_{\beta j}$ such that the C^2-normalized state $C_{\beta j}|\phi_{\beta j}\rangle$ almost coincides with the eigenstate $|\Phi_{\beta E_{\beta j}}\rangle$ for $r<R_0$ and its outer orbital might be continued to infinity as an energy-normalized shifted Coulomb wave.[40,41] The narrow wave packets fall off rapidly[40,41] for $r>R_0$ and this makes the present treatment similar to an R-matrix approach.[46] Indeed, the system may be considered "boxed" in a sphere with a soft boundary at $r=R_0$ and it is no wonder, therefore, that the variational narrow wave packets are practically coincident with the exact eigenfunctions having a node in R_0. The advantage of our choice is that all the matrix elements may be evaluated analytically.

In all the following, the basis-set functions employed are $|\varphi_{\beta j}\rangle=C_{\beta j}|\phi_{\beta j}\rangle$ with the understanding that $C_{\beta j}=1$ for the bound states (including all those in the zeroth subspace) and for the broad wave packets. In all the subsequent calculations the PWC eigenstates $|\Phi_{\beta E}\rangle$ are never explicitly needed: only their phase shifts and matrix elements are required both to compute the observables and to set up Eqs. (3).

The states referred to as narrow wave packets are such that, for all the matrix elements required by these calculations,

$$\langle f|\hat{O}|\Phi_{\beta E_{\beta j}}\rangle\approx\langle f|\hat{O}|\varphi_{\beta j}\rangle\ . \tag{7}$$

This is quite obvious when $|f\rangle$ is a localized state, while for $\langle\Phi_{\beta' E'}|\hat{H}-E|\Phi_{\beta'' E''}\rangle$, needed to set up Eqs. (3), a comment is appropriate. For $\beta'=\beta''$ these matrix elements are analytically dealt with before the discretization and the final equations are free from the associated divergencies. If $\beta'\neq\beta''$, the channel functions differ at least either in the ionic state or in the wave angular momentum; since the ionic states are chosen orthogonal and noninteracting, this means that no long-range integrand contributes to the expectation values of the one-electron Hamiltonian and of the monopole term $1/r_>$ of $1/r_{12}$. The worst case occurs with the dipole term $r_</r_>^2$, which involves contributions of the type

$$\int_0^\infty R_{\epsilon s}(r_>)R_{\epsilon p}(r_>)dr_>/r_>^2 \times \int_0^{r_>} R_{2s}(r_<)R_{2p}(r_<)r_<dr_< .$$

These integrals, however, are adequately reproduced if the states are correct up to about $R_0=200$ (see also the discussion of Salomonson *et al.*[36]). It must also be noted that each unit-normalized variational state $|\phi_{\beta j}\rangle$ may be associated with the energy interval $[\frac{1}{2}(E_{\beta j}+E_{\beta j-1}), \frac{1}{2}(E_{\beta j+1}+E_{\beta j})]$ in the sense

$$|\langle f|\hat{O}|\phi_{\beta j}\rangle|^2 \approx |\langle f|\hat{O}|\Phi_{\beta E_{\beta j}}\rangle|^2 \frac{E_{\beta j+1}-E_{\beta j-1}}{2}$$

at least when the integrand $f^*\hat{O}\Phi_{\beta E}$ is short range and weakly energy dependent.

D. Discretization procedure

The key requirement for the applicability of an L^2 technique is a regular behavior of all the quantities which are represented upon a finite basis set. The properties depending upon the continuous spectra of the projected Hamiltonians $\hat{Q}_\beta\hat{H}\hat{Q}_\beta$ must therefore have a smooth energy dependence. This implies that the PWC subspaces must not contain narrow shape resonances, a condition which is indeed satisfied for helium. If narrow shape resonances occur, appropriate single-channel localized representations of them should be projected out from the PWC subspaces and some suitable representations of them must be included in the zeroth subspace. The K-matrix technique, through the presence of $|\Phi_{\alpha E}\rangle$ and $P/(E-E')$ in expression (1) of the wave function $|\Psi_{\alpha E}\rangle$, takes care analytically of the fastest variations in the expansion coefficients and this allows the discretization on a basis set of the type described in Sec. II C.

The integrals in Eqs. (3) have been approximated by employing a cubic four-point Lagrange interpolation in the energy range associated with the narrow wave packets and treating all the remaining variational spectrum as if it were discrete. The coupled integral equations (3) are then turned into the following linear system for the elements $K^{\rm disc}_{\beta' j',\alpha E}$ of its discretized representation:[47]

$$\sum_{\beta',j'} [\mathbf{1}-\mathbf{V}(E)\mathbf{P}(E)]_{\beta j,\beta' j'} K^{\rm disc}_{\beta' j',\alpha E} = V^{\rm int}_{\beta j,\alpha E} \tag{8}$$

where

$$V_{\beta j,\beta' j'}(E)=(1-\delta_{\beta\beta'})\langle\varphi_{\beta j}|\hat{H}-E|\varphi_{\beta' j'}\rangle ,$$
$$V^{\rm int}_{\beta j,\alpha E}=(1-\delta_{\beta\alpha})\langle\varphi_{\beta j}|\hat{H}-E|\Phi_{\alpha E}\rangle^{\rm int} ,$$

and the superscript int denotes matrix elements which, by virtue of (7), have been interpolated from the grid supplied by the C^2-normalized narrow wave packets. The matrix $\mathbf{P}(E)$ takes care of the energy integration and has the almost diagonal structure[47] shown in Fig. 1. It is diagonal with elements $P_{\beta i,\beta i}=1/(E-E_{\beta i})$ for the functions considered discrete (i.e., bound states and broad wave packets) and it is almost diagonal over the narrow wave packets, where the overlapping 4×4 submatrices arise from the four-point interpolation.

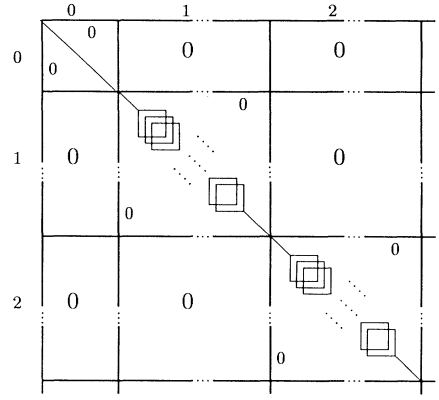

FIG. 1. Pattern of the matrix $\mathbf{P}(E)$ in the first few subspaces. $\mathbf{P}(E)$ is diagonal in correspondence to the states considered discrete, while it is a superposition of 4×4 matrices along the diagonal in correspondence to the narrow wave packets.

Since the contributions from the higher Rydberg series and from the high-energy spectrum are approximated by sums over the corresponding $|\varphi_{\beta j}\rangle$, this discretization is valid only if the contributions from these regions are small and weakly energy dependent. This means that the energy E in which we are interested must lie well inside the region covered by the narrow wave packets. In addition, a careful representation of many Rydberg states is necessary for reliable calculations close to a threshold.

E. Computational details

The ground state has been approximated by a large CI employing STO up to $l=6$. Since this is a standard calculation, it is sufficient to compare the calculated ground-state energy $-2.903\,592\,4$ with the "exact" nonrelativistic value $-2.903\,724\,377$ (Ref. 48) and the $l=6$ limit $-2.903\,643\,88$.[49]

The localized zeroth subset has been obtained by diagonalizing the Hamiltonian over a basis set of spin- and symmetry-adapted Slater determinants built with STO and hydrogenic orbitals up to $l=6$. This subset contains accurate localized representations of the bound and autoionizing states below the $N=3$ threshold up to an outer quantum number $n=8$ (these autoionizing states include three series converging to $N=2$ and five to $N=3$). It contains also a large number of localized wave packets which are needed to correlate the continuous variational states and lie above the $N=3$ threshold.

The present basis set includes all four PWC's ($1s\epsilon p$, $2s\epsilon p$, $2p\epsilon s$, and $2p\epsilon d$) which are open between the $N=2$ and $N=3$ thresholds, but no PWC's closed above $N=3$: these, as said before, are conveniently replaced by a large zeroth subset. The basis sets employed are such that each open PWC contains about ten accurate bound states, one or two wave packets in the higher Rydberg region, narrow wave packets up to a total energy $E\approx0.5$, and about 20 high-energy broad wave packets. The numbers of functions $|\varphi_{\beta j}\rangle$ in the localized zeroth subspace and in the four PWC's are, respectively, 197, 163, 105, 105, and 104.

The representation employed for the higher $N=2$ Rydberg series is rather coarse and one cannot expect the present calculations to be accurate at energies close to the $N=2$ threshold. The calculated cross sections show indeed spurious oscillations in the first 0.02 a.u. above the $N=2$ threshold. Reliable calculations in this region require better representations of the higher Rydberg series and more closely spaced narrow wave packets at very low wave energy. However, a basis set capable of reproducing accurately both the threshold and the resonance regions should be significantly larger and, in view of the structureless nature of the threshold region, would require an unjustified computational effort.

Owing to the nonorthogonality, the whole basis set was approximately linearly dependent, but the system solution through the LINPACK subroutines did not lead to numerical troubles. As a matter of fact, at all the energies studied the resulting discretized K matrix satisfied its determining equations (8) with excellent accuracy and the K matrix on the energy shell $\mathbf{K}(E)$ interpolated from it was almost exactly symmetric. In conclusion, it was possible to solve Eqs. (3) for any desired energy, obtaining very regular behaviors for all the quantities even sweeping the energy range of narrow resonances.

F. Analysis of the resonances

The determinant of the coefficient matrix $1-\mathbf{V}(E)\mathbf{P}(E)$ in Eq. (8) has a real zero near every eigenvalue E_{0j} of the localized zeroth subset which corresponds to an autoionizing state. While the general analysis may be tedious, this occurrence is easily shown if the variational state $|\varphi_{0j}\rangle$ represents a narrow isolated resonance. In this case, the discretized coefficient matrix may be conveniently written in the form

$$1-\mathbf{V}(E)\mathbf{P}(E)=\mathbf{A}^{(j)}(E)-\frac{\mathbf{V}^{(j)}(E)}{E-E_{0j}}$$

where the matrix $\mathbf{V}^{(j)}(E)$ is obtained from $\mathbf{V}(E)$ by deleting all the elements but those in the column corresponding to the autoionizing state. The determinant of this matrix is

$$\begin{aligned}\mathrm{Det}[1-\mathbf{V}(E)\mathbf{P}(E)]=&\{|A^{(j)}(E)|_{0j,0j}\}\\&-(E-E_{0j})^{-1}\\&\times\left\{\sum_{\beta,k}V_{\beta k,0j}(E)\right.\\&\left.\times|A^{(j)}(E)|_{\beta k,0j}\right\}\end{aligned}$$

where the $|A^{(j)}(E)|_{\beta k,0j}$ are the cofactors of $\mathbf{A}^{(j)}(E)$. Under the above hypotheses the terms in the two curly brackets are almost constant around E_{0j} and the first is much larger than the second. This implies that the determinant vanishes near E_{0j} and therefore the inverse matrix $[1-\mathbf{V}(E)\mathbf{P}(E)]^{-1}$ has a pole there. The above equation, in principle, may be employed to locate the pole. It may also be noted that the coefficient matrix diverges at $E=E_{0j}$; a careful analysis shows that this implies $K_{0j,\alpha E}\to 0$ when $E\to E_{0j}$, but the expansion coefficient $K_{0j,\alpha E}/(E-E_{0j})$ remains finite.

Around $E=E_{0j}$, the K matrix on the energy shell is therefore expected to have a series expansion of the form[50]

$$\mathbf{K}(E)=\sum_{i(\geq -1)}\mathbf{K}^{(i)}(E-E_0)^i$$

where $E_0\approx E_{0j}$ is a real energy. For all the resonances examined, it was found with excellent approximation that

$$\mathbf{K}^{(-1)}=\mathbf{a}_0^{\dagger}\mathbf{a}_0\Gamma_0/2\pi$$

where $\mathbf{a}_0$ is a normalized row vector ($\sum_\gamma |a_{0\gamma}|^2=1$). This implies a Wigner-type pole of the scattering matrix,[50] i.e.,

$$\mathbf{S}(E)=\frac{\mathbf{a}_r^{\dagger}\mathbf{a}_r}{E-E_R}+\sum_{i(\geq 0)}\mathbf{S}^{(i)}(E-E_R)^i \tag{9}$$

where $\mathbf{a}_r$ is a normalized row vector. The complex pole $E_R=E_r-i\Gamma_r/2$ of $\mathbf{S}(E)$ gives the position E_r and the width Γ_r of the resonance, while $b_\gamma=|\mathbf{a}_{r\gamma}|^2$ are the branching ratios, i.e., the relative probability of decaying in the γth channel.[50] For a resonance of this type, only one eigenvalue of $\mathbf{K}(E)$ may diverge, while the other ones must have a regular behavior. The diverging eigenvalue $\Lambda_{\mathrm{div}}(E)$ may be expanded in the form

$$\Lambda_{\mathrm{div}}(E)=\frac{\Gamma_0}{2\pi(E-E_0)}+\sum_{i(\geq 0)}\Lambda^{(i)}(E-E_0)^i$$

and, according to Eq. (6), the pole of $\mathbf{S}(E)$ is found by solving

$$1+i\pi\Lambda_{\mathrm{div}}(E)=0\ .$$

It is a widespread belief that for a narrow resonance $\Gamma_0\approx\Gamma_r$ and $\mathbf{a}_0\approx\mathbf{a}_r$, but the above formula shows that this is not generally true. Indeed, at a narrow resonance E_R-E_0 is small and this implies that $\Lambda^{(i)}(E_R-E_0)^i$ is small for $i>0$, but not for $i=0$. It appears that often the $\Lambda^{(0)}$ coefficient is essential for obtaining a reliable S-matrix pole, while those beyond $\Lambda^{(1)}$ give only negligible corrections. This is clearly demonstrated by the 2_4 resonance, for which this method yielded a width of 6.83×10^{-5} employing only the leading term and of 3.22×10^{-5} with an accurate polynomial fit of $\Lambda_{\mathrm{div}}(E)$. It is interesting to compare these figures with the value 3.18×10^{-5} given by Lorentzian-fit method explained below and with the golden-rule estimate 0.89×10^{-5}

$$\Gamma_{\mathrm{gold}}=2\pi\sum_\gamma|\langle\Phi_{\gamma E_{0j}}|\hat{H}-E_{0j}|\varphi_{0j}\rangle|^2\ .$$

This poor result was not unexpected in view of our previous work, where an improved version of this rule was proposed.[40,41]

An alternative way of analyzing the resonances is founded upon the consideration that, if a reliable localized approximation $|\varphi_{0j}\rangle$ to an isolated autoionizing state exists, its density $D_j(E)$ in the continuous eigen-

states

$$D_j(E)=\sum_\gamma |\langle \Psi^{(\pm)}_{\gamma E}|\varphi_{0j}\rangle|^2=\sum_\gamma D_{\gamma j}(E)$$

should resemble a Lorentzian centered in E_r.[43] The fit of $D_j(E)$ yields therefore the position and the width of the resonance, while the areas subtended by the $D_{\gamma j}(E)$ give the branching ratios.

Finally, the parameters for the lowest (1_3 or $3s3p$) resonance, which has been the subject of careful experimental studies,[3,8,15,16] have been obtained also by fitting the photoionization cross section $\sigma(E)$ by the many-channel Fano-Cooper formula[51]

$$\sigma(E)=\sigma_0[1+a(E-E_0)]\left[\rho^2\frac{(q+\epsilon)^2}{1+\epsilon^2}+1-\rho^2\right];$$

$$\epsilon=\frac{2(E-E_0)}{\Gamma} \quad (10)$$

in which a linear variation of the background cross section $\sigma_b(E)=\sigma_0[1+a(E-E_0)]$ is assumed.

All these techniques assume the knowledge of the continuum properties at several energies in the neighborhood of the resonance. The capability of the present method to reproduce correctly the resonance behavior is shown in Fig. 2, which reports the $2s\epsilon p$ partial cross section across the narrow 2_4 resonance as calculated with the length gauge (LG) [the velocity gauge (VG) results are almost indistinguishable on this scale].

The search for very narrow resonances is greatly simplified since the eigenvalues of the zeroth set (eventually with the first-order Fano correction[43]) and the golden-rule widths represent reliable starting points. This avoids the laborious searching often required in these cases by the most usual close-coupling techniques, where these starting points are not easily available.

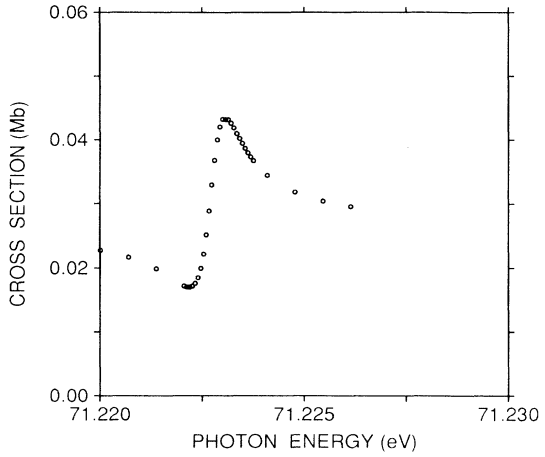

FIG. 2. Details of the length gauge $2s\epsilon p$ photoionization cross section around the 2_4 resonance.

G. Cross sections and asymmetry parameters

The γ-channel cross section is simply the contribution due to the $|\Psi^{(-)}_{\gamma E}\rangle$ state and the total $N_I L_I S_I$ cross section (i.e., to the ion in a given level) is clearly the sum over the channels associated with this ionic level.

Also, in view of future applications, it appears to be worth reporting here the general expression of the asymmetry parameter $\beta_{N_I L_I S_I}$ for the photoionization which leaves the ion in the $N_I L_I S_I$ level starting from an arbitrary initial $N_0 L_0 S_0$ level. Denoting the states of the initial level by $|\Psi_{N_0 L_0 S_0; M_L M_S}\rangle$ and the final states involved in the photoionization process by $|\Psi^{(-)}_{EN_I L_I S_I l_i L_i S_0; M_L M_S}\rangle$ (where l_i and L_i are the wave and total orbital angular momenta), the asymmetry parameter $\beta_{N_I L_I S_I}$ may be expressed as

$$\beta_{N_I L_I S_I}=\sum_{ij}(-1)^{L_0+L_I+l_i+l_j+L_i+L_j}[(2l_i+1)(2l_j+1)(2L_i+1)(2L_j+1)]^{1/2}$$
$$\times C(112;000)C(l_i l_j 2;000)W(1L_i 1L_j;L_0 2)W(l_i L_i l_j L_j;L_I 2)$$
$$\times\langle N_0 L_0 S_0\|\hat{O}\|EN_I L_I S_I l_i L_i S_0\rangle^*\langle N_0 L_0 S_0\|\hat{O}\|EN_I L_I S_I l_j L_j S_0\rangle$$
$$\times\left[\frac{1}{3}\sum_i |\langle N_0 L_0 S_0\|\hat{O}\|EN_I L_I S_I l_i L_i S_0\rangle|^2\right]^{-1}$$

where C and W are the Clebsch-Gordan and Racah coefficients, respectively, and

$$\langle N_0 L_0 S_0\|\hat{O}\|EN_I L_I S_I l_i L_i S_0\rangle$$

the reduced matrix elements between the initial and the final states. All these quantities follow the Rose conventions.[52]

The asymmetry parameter for the processes leaving He^+ in an ns level has the constant value $\beta_{ns}=2$, while β_{2p} is energy dependent, owing to the interaction of the $2p\epsilon s$ and $2p\epsilon d$ channels. Since the $2s$ and $2p$ ion levels are almost degenerate, the separate angular distributions of the corresponding photoelectrons have not yet been resolved, but several authors[9,11,12,14,16] have measured the distribution for the totality of the $N=2$ photoelectrons. The asymmetry parameter for this process is

$$\beta_2=(\sigma_{2s}\beta_{2s}+\sigma_{2p}\beta_{2p})/(\sigma_{2s}+\sigma_{2p}) .$$

All the present calculations have been performed with both the LG and VG forms of the transition operator and

the gauge invariance is generally quite good. The VG form appears, however, superior since it is less sensitive to small imprecisions in the variational states; in particular the VG results stabilized very rapidly during the preliminary runs with limited bases.

III. RESULTS AND DISCUSSION

All energies are expressed in eV and the photoionization cross sections in megabarns (Mb). The energy conversion factor, which takes care of the reduced mass

TABLE I. Calculated positions E and widths Γ for the resonances converging to the $N=3$ threshold. The resonances' labels A and K_n follow the notation of Lin (Ref. 32). Upper line: S-matrix results, lower line: Lorentzian-fit results (see text). $a[-b]$ means $a\times10^{-b}$.

				Branching ratios			
A	K_n	E (eV)	Γ (eV)	$1s\epsilon p$	$2s\epsilon p$	$2p\epsilon s$	$2p\epsilon d$
1	1_3	69.8793	1.84[−1]	0.019	0.141	0.532	0.308
		69.8770	1.84[−1]	0.019	0.136	0.528	0.317
−1	2_4	71.2264	8.75[−4]	0.002	0.456	0.389	0.153
		71.2264	8.65[−4]	0.002	0.458	0.389	0.151
1	-1_3	71.3204	3.74[−2]	0.002	0.157	0.043	0.798
		71.3196	3.67[−2]	0.003	0.152	0.043	0.802
1	1_4	71.6372	8.18[−2]	0.026	0.141	0.534	0.299
		71.6358	7.84[−2]	0.023	0.149	0.541	0.287
−1	0_4	71.7312	5.84[−4]	0.001	0.200	0.029	0.770
		71.7312	5.52[−4]	0.001	0.208	0.039	0.752
−1	2_5	72.0016	5.95[−4]	0.001	0.426	0.428	0.145
		72.0016	5.80[−4]	0.001	0.427	0.430	0.142
1	-1_4	72.1712	1.82[−2]	0.004	0.149	0.320	0.527
		72.1683	2.19[−2]	0.009	0.073	0.271	0.647
1	1_5	72.1872	2.91[−2]	0.021	0.231	0.531	0.217
		72.1832	2.08[−2]	0.018	0.326	0.472	0.184
−1	0_5	72.2539	2.75[−4]	0.001	0.182	0.031	0.786
		72.2539	2.72[−4]	0.001	0.198	0.039	0.762
0	-2_4	72.3346	1.51[−6]	0.004	0.131	0.032	0.833
		72.3346	1.22[−6]	0.003	0.128	0.039	0.830
−1	2_6	72.3549	3.59[−4]	0.001	0.412	0.447	0.140
		72.3549	3.50[−4]	0.001	0.415	0.448	0.136
1	1_6	72.4536	2.06[−2]	0.012	0.208	0.472	0.308
		72.4492	2.11[−2]	0.016	0.058	0.393	0.533
1	-1_5	72.4580	5.95[−3]	0.019	0.475	0.395	0.111
		72.4582	5.11[−3]	0.019	0.483	0.383	0.115
−1	0_6	72.4951	1.58[−4]	0.001	0.178	0.033	0.788
		72.4951	1.60[−4]	0.001	0.192	0.040	0.767
0	-2_5	72.5309	5.02[−6]	0.002	0.128	0.011	0.859
		72.5309	5.17[−6]	0.002	0.139	0.017	0.842
−1	2_7	72.5444	2.26[−4]	0.000	0.409	0.452	0.139
		72.5444	2.17[−4]	0.000	0.410	0.457	0.133
1	1_7	72.6026	1.43[−2]	0.017	0.151	0.490	0.342
		72.6009	1.39[−2]	0.017	0.048	0.394	0.541
1	-1_6	72.6075	2.69[−3]	0.020	0.535	0.331	0.114
		72.6075	2.52[−3]	0.021	0.534	0.322	0.123
−1	0_7	72.6294	1.14[−4]	0.002	0.156	0.025	0.817
		72.6294	1.08[−4]	0.002	0.166	0.037	0.795
0	-2_6	72.6486	6.69[−6]	0.003	0.093	0.033	0.871
		72.6486	6.99[−6]	0.004	0.102	0.042	0.852
−1	2_8	72.6574	1.46[−4]	0.001	0.427	0.417	0.155
		72.6574	1.39[−4]	0.001	0.428	0.421	0.150
1	1_8	72.6948	1.01[−2]	0.018	0.140	0.494	0.348
		72.6938	9.96[−3]	0.018	0.054	0.421	0.507
1	-1_7	72.6982	1.60[−3]	0.020	0.546	0.287	0.147
		72.6982	1.54[−3]	0.020	0.543	0.282	0.155
−1	0_8	72.7128	1.32[−4]	0.006	0.044	0.084	0.866
		72.7128	1.35[−4]	0.007	0.056	0.095	0.842

correction, is 1 a.u.(^{4}He)=27.207 696 eV. The difference with the factor employed in our previous work[40] is due to the change in the recommended energy conversion factors.[53] It is, however, worth noting that, as pointed out by Bhatia and Temkin,[54] this correction is appropriate for comparing the theoretical results with photoabsorption experiments, but not with energy loss (electron impact) values. The calculated ground-state energy is −79.0001 eV, versus the "exact" nonrelativistic value −79.0037 eV (Ref. 48) and the experimental value −79.0052 eV.[55] The resonance positions will be reported to four decimal places; this precision is unjustified for the excitation energy, but meaningful for the relative positions and for comparing the results of the different analyses.

The present calculations do not include the quantities needed to classify the autoionizing states according to the Herrick and Sinanoglu[20] scheme, but it was nevertheless possible to arrange the resonances in series by grouping them accordingly to the regularities of the following

TABLE II. Comparison of the present S-matrix results for the resonances with theoretical and experimental data. Upper line, position (eV above the ground state); lower line, width Γ (eV). The resonances' labels A and K_n follow the notation of Lin (Ref. 32). The uncertainty on the last digit of the reported data is in parentheses. $a[-b]$ means $a\times10^{-b}$.

			Theoretical[a]			Experimental	
A	K_n	Present	Ref. 18[b]	Ref. 30[c]	Ref. 36[d]	Ref. 8[e]	Ref. 16[f]
1	1_3[g]	69.8793	69.8666	69.8721		69.917(12)	69.880(22)
		1.84[−1]		1.9[−1]		0.178(12)	0.180(15)
−1	2_4	71.2264	71.2217	71.2236	71.230		
		8.75[−4]		7.6[−4]	9.05[−4]		
1	-1_3[h]	71.3204	71.3083	71.3086		71.30(4)	71.261(30)
		3.74[−2]		3.9[−2]		≈0.07	0.073(15)
1	1_4	71.6372	71.6269	71.6242		71.601(18)	71.625(30)
		8.18[−2]		8.4[−2]		0.096(15)	
−1	0_4	71.7312	71.7255	71.7217	71.745		
		5.84[−4]		3.[−4]	1.16[−3]		
−1	2_5	72.0016	71.9993	71.9996	72.000		
		5.95[−4]		4.[−4]	5.92[−4]		
1	-1_4	72.1712	72.1689	72.1582			
		1.82[−2]		1.4[−2]			
1	1_5	72.1872	72.1886	72.1807		72.181(15)	72.174(30)
		2.91[−2]		3.3[−2]		0.067(15)	
−1	0_5	72.2539	72.2560	72.2484	72.259		
		2.75[−4]			5.51[−4]		
0	-2_4	72.3346	72.3402	72.3229	72.3535		
		1.51[−6]			8.9[−5]		
−1	2_6	72.3549	72.3549		72.3549		
		3.59[−4]			3.6[−4]		
1	1_6	72.4536	72.4603			72.453(11)	72.423(30)
		2.06[−2]				0.038(15)	
1	-1_5	72.4580	72.4680				
		5.95[−3]					
−1	0_6	72.4951	72.4977		72.498		
		1.58[−4]			2.99[−4]		
0	-2_5	72.5309	72.5378		72.5461		
		5.02[−6]			6.22[−5]		
−1	2_7	72.5444	72.5575		72.5441		
		2.26[−4]			2.2[−4]		
1	1_7	72.6026	72.6275			72.59(1)	72.561(30)
1	1_8	72.6948				72.67(1)	72.640(30)

[a]With respect to the "exact" nonrelativistic ground state −79.0037 (Ref. 48).
[b]Feshbach method.
[c]Complex stabilization with Hylleraas functions.
[d]Nine-channel many-body perturbative K matrix.
[e]Analysis of the $N=2$ cross section. Terms in parentheses represent statistical uncertainties only; systematic error ±0.009 eV for positions, ±0.008 eV for widths.
[f]Analysis of the $N=2$ differential cross section. Energy calibration ±0.015 eV.
[g]Further data for the 1_3 resonance: $E=69.8891$,[a] $\Gamma=0.189$ (nine-state close coupling, Ref. 25); $E=69.88$[a] $\Gamma=0.18$ (ten-channel R matrix, Ref. 35); $E=69.919(7)$, $\Gamma=0.132(14)$, $\Gamma=0.132(14)$ (experiment, Ref. 3); $E=69.914(15)$, $\Gamma=0.200(20)$ (experiment, Ref. 15, energy calibration ±0.010 eV).
[h]Further data for the -1_3 resonance: $E=71.3311$,[a] $\Gamma=0.030$ (nine-state close coupling, Ref. 25).

properties: effective quantum numbers n^*, widths (which scale roughly as $1/n^{*3}$), branching ratios, and projections onto the subspaces of $sp,pd,df,\ldots$ configurations. The present results for the resonances are fully presented in Table I, while in Table II energies and widths obtained by the S-matrix method are compared with the most accurate and comprehensive theoretical and experimental results. For ease of comparison with other theoretical work, the resonance positions are all expressed with respect to the "exact" nonrelativistic ground state.

The ordering obtained agrees with that of Chung[18] and of Herrick and Sinanoglu[20] and does not support the different classification proposed by Ho[26] for the sixth resonance. Indeed, Ho classifies it as -2_4 instead of 2_5 as Herrick and Sinanoglu do; as shown in Table I it correlates with the second resonance, which is classified as 2_4 by both authors.

The resonances -2_n and 2_{n+2} are very close to each other for $n \geq 4$, but they are very narrow and may still be considered isolated. It must be noted that the -2_5 resonance is found to be about four times larger than the -2_4 and the -2_6 even larger. On the contrary, Salomonson *et al.*[36] found the -2_5 resonance narrower than the -2_4 one, but their widths are more than ten times greater than ours. No other accurate calculations of these widths exist. In view of the quality of our zeroth subset, this means that, if our findings are spurious, the calculation of these widths is a very critical computational problem.

In agreement with Chung[18] and with Herrick and Sinanoglu[20] the -2_{n+2} resonance is predicted to lie below the 2_n at least up to $n=6$, while the recent calculations of Salomonson *et al.*[36] find the -2_5 above the 2_7. The relative positions of the helium narrow resonances provide an exacting computational task already below the $N=2$ threshold. Indeed, as discussed elsewhere,[40] a very good account of the electronic correlation is required to obtain the correct order of the $(N=2)$ -1_3 and 1_4 resonances (perhaps best known as $2,3c$ and $2,4b$ in the phenomenological notation of Lipsky and Conneely[32] or as $2p3d$ and $2,4-$ in the Fano-Cooper one[32]). It appears that a basis set including only the open $N=1$ and the three closed $N=2$ channels is not sufficient to reproduce the correct order of these $N=2$ resonances, and that also the inclusion of the five closed $N=3$ channels[36] is required to do this. In this context, it should be recalled that the present calculations implicitly employ, through the zeroth subspace, a large number of closed channels.

The agreement with the theoretical widths of Ho,[26,30] obtained with Hylleraas-type wave functions and the complex stabilization method, is satisfactory. The largest differences occur for the 0_4 and 2_5 resonances for which Ho gives the width with only one significant digit, i.e., with an uncertainty of 25%. The agreement with the calculations of Salomonson *et al.*[36] is less good, in particular for the 0_n and -2_n resonances. This is not surprising if one considers that their calculations are essentially of K-matrix type with orthogonality constraints on the subspaces: these authors cannot employ a correlated zeroth subspace as in the present work but introduce the five $N=3$ closed channels ($3s\epsilon p$, $3p\epsilon s$, $3p\epsilon d$, $3d\epsilon p$, and $3d\epsilon f$). Their basis set, unlike ours, does not include fg, gh, and hi configurations which contribute noticeably to the resonances of the 0_n and -2_n series.

The data reported in Table II show also that there is no obvious systematic trend in the differences among the theoretical positions of the autoionizing states, and that the present calculations are in good agreement with the experimental data of Zubek *et al.*[16] As apparent from Tables I and II, the resonances -1_n and 1_{n+1} lie rather close for $n \geq 4$ and their distance is comparable with their widths. Thus they cannot be considered isolated and it is not surprising that the two methods employed in this work for analyzing the resonances give for them the greatest differences. In fact, the Lorentzian-fit method assumes truly isolated resonances, while the search for the poles of the S-matrix according to Eq. (9) may handle more difficult cases. It may also be noted that at $n=5$ these resonances reverse their relative positions. The widths of the four lowest 1_n resonances have been determined by Woodruff and Samson[8] from the analysis of the $N=2$ cross section in terms of a Shore[56] profile. The

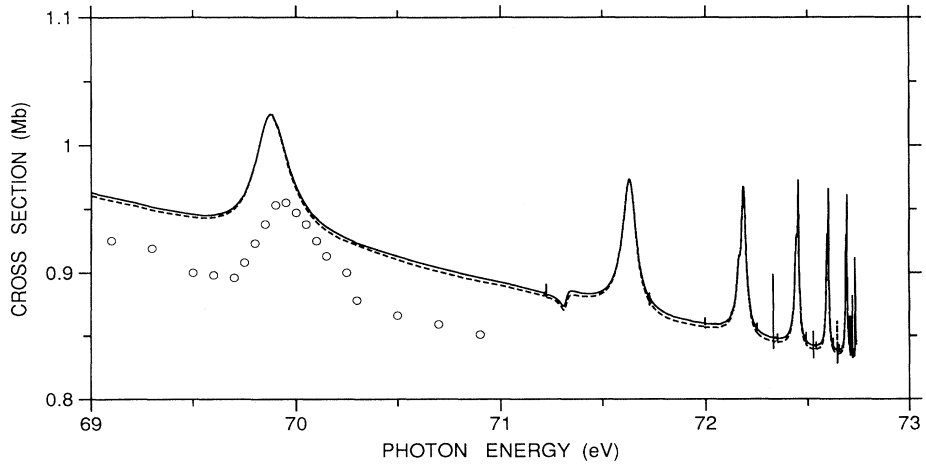

FIG. 3. Partial $1s\epsilon p$ cross section $\sigma_{1s\epsilon p}$. Solid line, LG results; dashed line, VG results; ○, experimental results of Lindle *et al.* (Ref. 14).

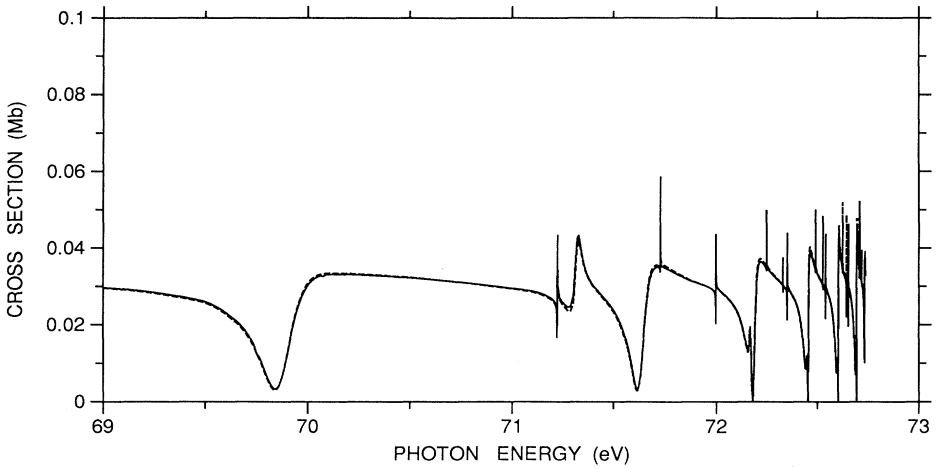

FIG. 4. Partial $2s\epsilon p$ cross section $\sigma_{2s\epsilon p}$. Solid line, LG results; dashed line, VG results.

present widths are in good agreement with their experimental counterparts for the 1_3 and 1_4 resonances, while for the 1_5 and 1_6 they are significantly smaller. Indeed, the experimental widths for these last two resonances are in fair agreement with the theoretical estimates for the two unresolved pairs $(-1_4;1_5)$ and $(1_6;-1_5)$.

For the -1_3 resonance the present width $\Gamma\approx 0.037$ is about one half of the experimental value[8,16] $\Gamma\approx 0.07$. While the datum of Woodruff and Samson[8] is simply an estimate this resonance appearing only as a faint shoulder in their recorded spectrum, the value given by Zubek *et al.*[16] might refer to the unresolved pair 2_4 and -1_3 as explained below. Anyway, in comparing these theoretical data with their counterparts derived from the experimental cross sections, one should not forget that these last parameters are extracted by phenomenological fitting formulas. For the 1_3 resonance (often called $3s3p$), this point will be further discussed below.

Figures 3–9 report the calculated partial ($\sigma_{1s}=\sigma_{1s\epsilon p}$, $\sigma_{2s}=\sigma_{2s\epsilon p}$, $\sigma_{2p\epsilon s}$, $\sigma_{2p\epsilon d}$, $\sigma_{2p}=\sigma_{2p\epsilon s}+\sigma_{2p\epsilon d}$, and $\sigma_2=\sigma_{2s}+\sigma_{2p}$) and total photoionization cross sections in the range 69–72.75 eV, together (when available) with the experimental data of Lindle *et al.*[11,14] and show an excellent gauge invariance. Below 69 eV, the cross sections are very smooth and appear of relatively minor interest; above 72.75 eV the employed basis set does not contain functions suitable to represent the resonances. It must be observed, however, that the crowding of the resonances between this energy and the $N=3$ threshold at 72.96 eV makes hopeless here any comparison with experiment.

Several authors[19,23,24,29,31,34–36] have calculated the helium photoionization cross section above the $N=2$ threshold, but in many cases these calculations were only intended to supply coarse information up to about 120–200 eV and do not show the resonance structure. The cross sections calculated by Salomonson *et al.*,[36] at least below 72 eV, are in excellent agreement with the present ones, including several fine details. For the $N=1$ cross section, however, the present results have a better

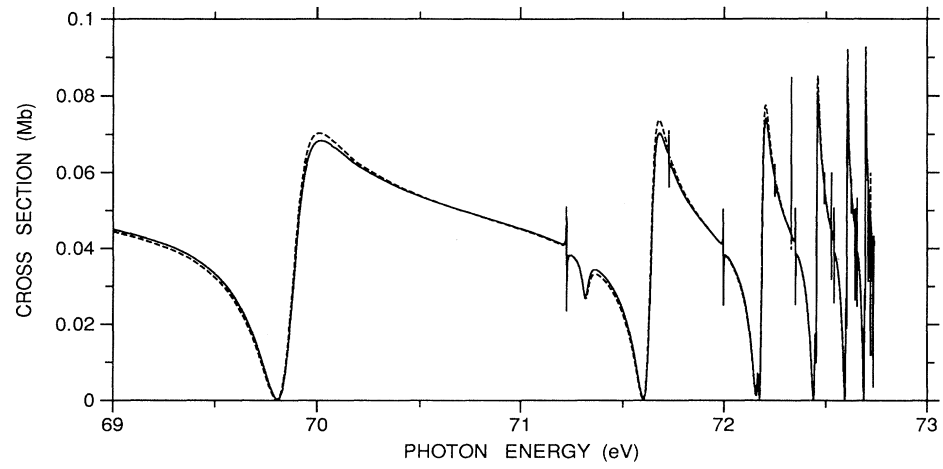

FIG. 5. Partial $2p\epsilon s$ cross section $\sigma_{2p\epsilon s}$. Solid line, LG results; dashed line, VG results.

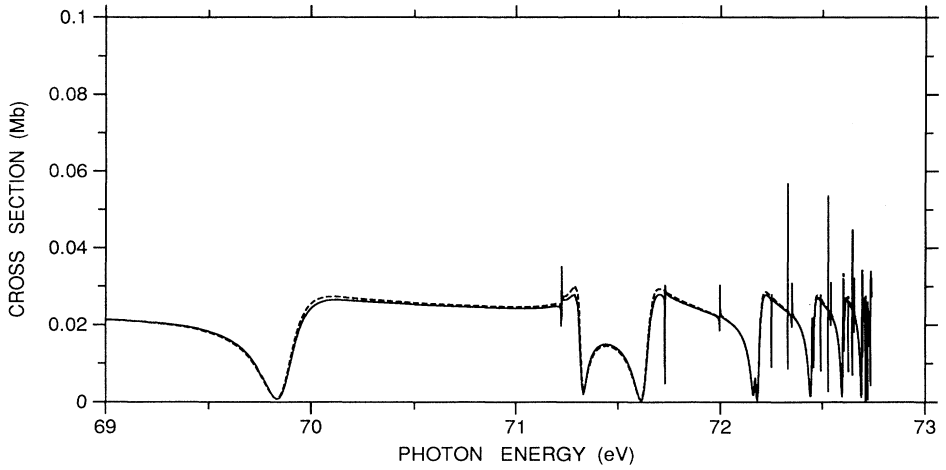

FIG. 6. Partial $2p\epsilon d$ cross section $\sigma_{2p\epsilon d}$. Solid line, LG results; dashed line, VG results.

gauge invariance and are in fair agreement with the average of their LG and VG results. Larger differences are found with the calculations of Hayes and Scott[35] and of Burkov *et al.*[34] The present calculations extend those of Salomonson *et al.*[36] towards the $N=3$ threshold by only 0.15 eV, but this narrow energy range contains eight autoionizing states. As explained in Sec. II E, the basis set was chosen for describing accurately only the resonance region and as a consequence the present results are not very accurate from the $N=2$ threshold at 65.40 up to 66 eV. The cross sections below 69 eV, however, are very smooth and may be safely extrapolated to the threshold, yielding in LG (VG) 1.117 (1.112), 0.026 (0.026), 0.060 (0.059), and 0.022 (0.022) Mb for the four channels $1s\epsilon p$, $2s\epsilon p$, $2p\epsilon s$, and $2p\epsilon d$ and a total cross section 1.225 (1.219) Mb. At 66.8 eV the present total cross section is 1.161 (1.157) Mb, versus the experimental value 1.109±3% Mb of Watson.[2] At 67.02 and 68.88 eV, it is 1.152 (1.149) and 1.065 (1.062) Mb, to be compared with the recommended experimental values 1.08±5% and 1.02±5% Mb of West and Marr.[4]

Figure 10 reports the present calculated total cross section across the 1_3 resonance, together with two recent experimental results. Both experimental works normalize their results by employing the "off-resonance" cross-section value 1.02 Mb given by West and Marr[4] at 68.88 eV, but in a different way. Lindle *et al.*[11,14] normalize the observed cross section to this value, while Kossmann *et al.*[15] normalize the background cross section, i.e., the factor $\sigma_b(E)$ of Eq. (10). The difference originates from the fact that the resonance structure is not seen in the experiment of West and Marr,[4] who have a resolution of 2 Å, i.e., about 0.6 eV. However, if their value is assumed to be a (symmetrically weighted) average in the range 68.6–69.2 eV, the shape of the total cross section implies that at 68.88 eV $\sigma=1.02$ Mb represents a lower bound. In view of this, both the experimental results of Fig. 10 should be shifted slightly upward, thus improving the agreement with the present cross section. At 68.88 eV, the present calculations yield a LG (VG) total cross sec-

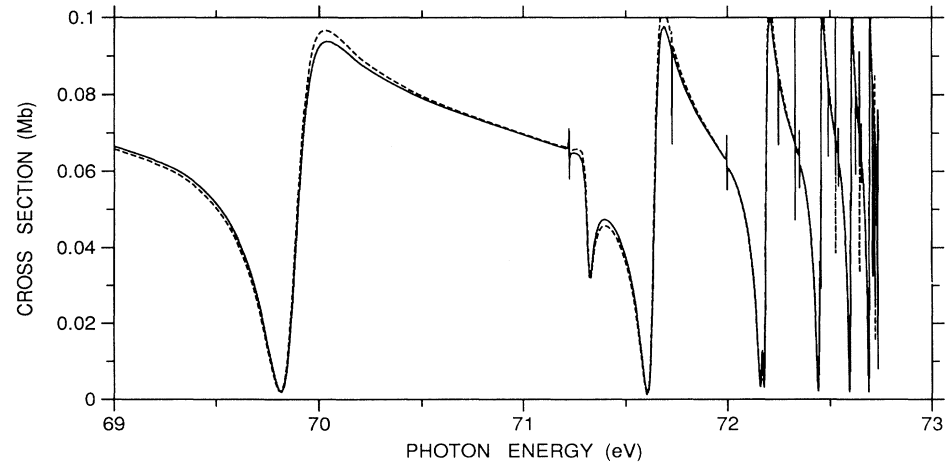

FIG. 7. Partial $2p$ cross section $\sigma_{2p}=\sigma_{2p\epsilon s}+\sigma_{2p\epsilon d}$. Solid line, LG results; dashed line, VG results.

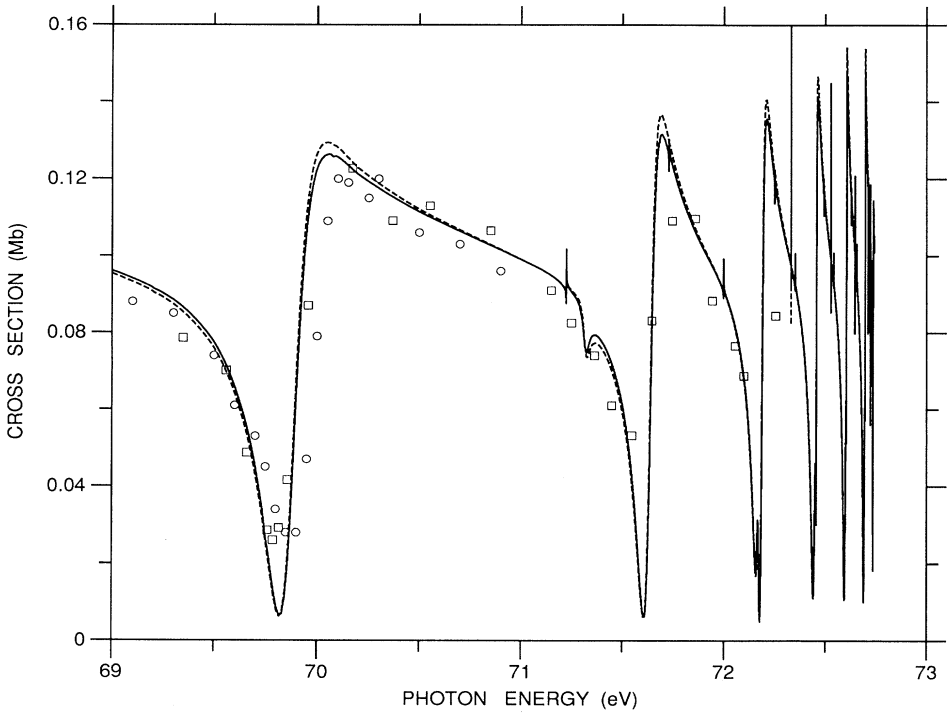

FIG. 8. Total $N=2$ cross section $\sigma_2=\sigma_{2s}+\sigma_{2p}$. Solid line, LG results; dashed line, VG results; □, experimental results of Lindle *et al.* (Ref. 11); ○, experimental results of Lindle *et al.* (Ref. 14).

tion of 1.065 (1.062) Mb, in good agreement with the theoretical values 1.05 (1.08) Mb of Salomonson *et al.*[36] (extrapolated from their Fig. 13) and 1.1 of Hayes and Scott.[35] The recommended value of West and Marr[4] appears therefore to be slightly too low; however, the present results lie inside its maximum stated error (±5%). Table III reports the parameters obtained by fitting the $N=1$, $N=2$, and total cross sections with the Fano-Cooper formula (10) between 69 and 71 eV (146 calculated points). These results were obtained by optimizing simultaneously all six parameters of Eq. (10), but fits of almost comparable quality were obtained also with one or more parameters kept fixed. In particular, this was verified both when the position and the width were fixed to the calculated values reported in Table I and when q and ρ^2 were fixed to the experimental values. This means that the parameters are strongly correlated and thus their physical meaning is seriously undermined. There has been some debate on the relative phases (i.e., the q signs) of the $N=1$ and $N=2$ cross sections.[8,11,14] In agreement

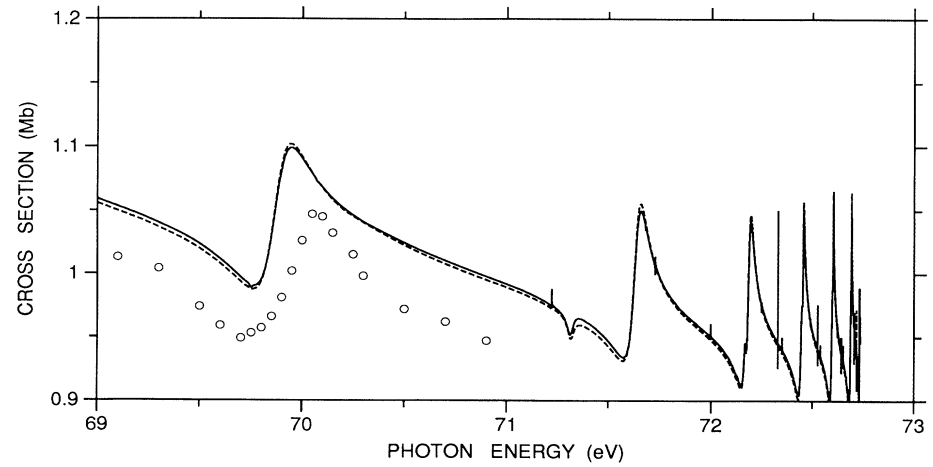

FIG. 9. Total cross section $\sigma=\sigma_{1s\epsilon p}+\sigma_2$. Solid line, LG results; dashed line, VG results; ○, experimental results of Lindle *et al.* (Ref. 14).

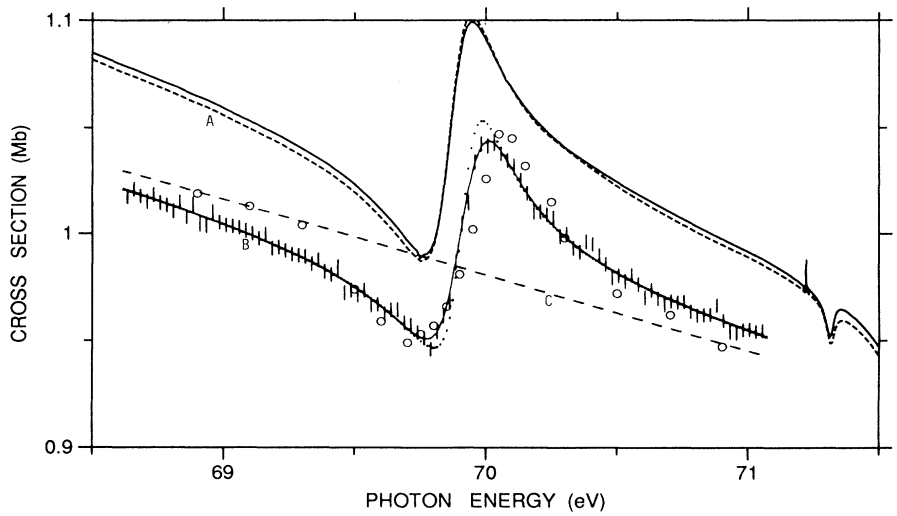

FIG. 10. Detail of the total cross section around the 1_3 resonance. Curve A: this work, LG (solid line) and VG (dashed line) results. Curve B: experimental results of Kossmann *et al.* (Ref. 15) (error bars) and their interpolation without (solid line) and with (dotted line) correction for the monochromator band pass. Curve C: experimental results of Kossmann *et al.* (Ref. 15), background cross section as defined by Eq. (10) (dashed line). ○: experimental results of Lindle *et al.* (Ref. 14).

with Lindle *et al.*,[11,14] we found both q positive, i.e., both the $N=1$ and $N=2$ cross sections reach their maximum above the resonance position. For a shape like that of the $N=1$ cross section, the q value has hardly a definite meaning, so the large difference with the experimental result is not surprising.

The branching ratios for this resonance, 0.019, 0.141, 0.532, and 0.308 (S-matrix method), are in good agreement with the experimental values 0.02, 0.12, 0.58, and 0.28 given by Lindle *et al.*[14]

The present calculations show that the σ_{2p} dominates over the σ_{2s} at almost all the energies examined, with exceptions only at its minima. This is in agreement with nearly all the calculations and all the experimental evi-

TABLE III. Fano-Cooper parameters for the 1_3 resonance as defined by Eq. (10). The uncertainty on the last digit of the reported data is in parentheses.

	E_0 (eV)	Γ (eV)	q	ρ^2	σ_0 (Mb)	a (eV^{-1})
	Parameters from the total cross section					
This work, LG	69.874	0.196	1.19	0.047	1.034	−0.0448
This work, VG	69.874	0.197	1.24	0.047	1.031	−0.0448
Dhez and Ederer (Ref. 3)[a]	69.919(7)	0.132(14)	1.36(20)	0.012(3)	0.957(30)	0(fixed)
Lindle *et al.* (Ref. 14)	69.917[b]	0.178[b]	1.30(5)	0.057(5)	0.991(30)[c]	−0.0480
Kossmann *et al.* (Ref. 15)[d]	69.914(15)	0.200(20)	1.32(5)	0.043(5)	0.983(25)	−0.0366
	Parameters from the $N=2$ cross section					
This work, LG	69.875	0.192	0.510	0.938	0.103	−0.0075
This work, VG	69.875	0.192	0.542	0.939	0.103	−0.0077
Woodruff and Samson (Ref. 8)[e]	69.917(12)	0.178(12)	0.48(9)	0.98(26)	0.084(21)	0(fixed)
Lindle *et al.* (Refs. 11 and 14)	69.917[b]	0.178[b]	0.70(6)	0.89(8)	0.097(5)	−0.0175
	Parameters from the $N=1$ cross section					
This work, LG	69.873	0.190	9.81	0.001	0.931	−0.0371
This work, VG	69.873	0.190	10.96	0.001	0.929	−0.0368
Lindle *et al.* (Ref. 11)	69.917[b]	0.178[b]	1.1(3)	0.046(30)	0.891(20)	−0.0317
Lindle *et al.* (Ref. 14)	69.917[b]	0.178[b]	3.0(1)	0.012(4)	0.893(5)	−0.0549

[a]From Ref. 15.
[b]Taken from Ref. 8.
[c]Cross section normalized upon the value of West and Marr (Ref. 4) at 68.88 eV.
[d]Energy calibration ±0.010 eV; background cross section normalized upon the value of West and Marr (Ref. 4) at 68.88 eV.
[e]From the results of a multiresonance Shore fit. Figures in parentheses represent statistical uncertainties only. Systematic errors ±0.009 eV for position, ±0.008 eV for width.

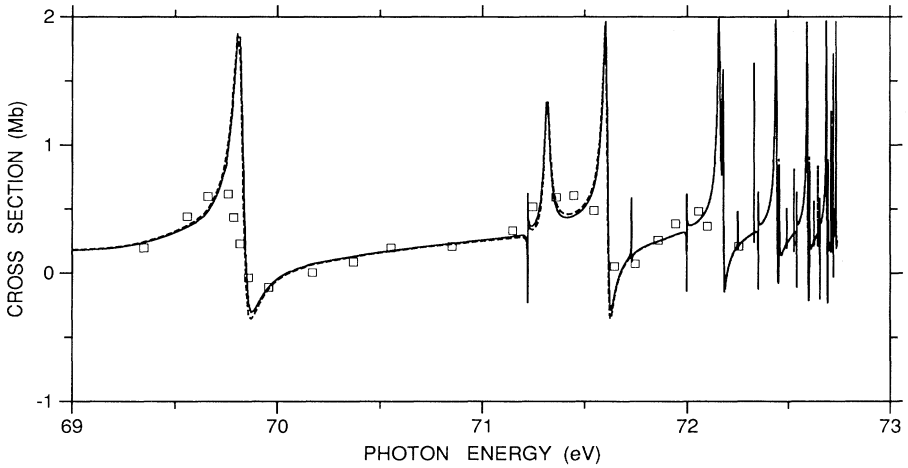

FIG. 11. Asymmetry parameter β_2 for the photoionization to the $N=2$ level. Solid line, LG results; dashed line, VG results; □, experimental results of Lindle *et al.* (Ref. 11).

dence. Most of the latter is, however, indirect, since it is obtained from measured values of the asymmetry parameter β_2 and theoretical estimates of β_{2p}. So far, the only experiment which has resolved the $2s$ and $2p$ cross sections is that of Woodruff and Samson,[8] who analyzed the $2p \rightarrow 1s$ fluorescence at 304 Å in the presence of a static electric field. At 67 eV they found $\sigma_{2s}=0.0299\pm0.0005$ Mb and $\sigma_{2p}=0.0741\pm0.0005$ Mb (with a probable systematic error of $\pm12\%$), in good agreement with the present LG (VG) results $\sigma_{2s}=0.0295$ (0.0295) Mb and $\sigma_{2p}=0.0770$ (0.0765) Mb. At 70.1 eV these authors report, in their Table I, $\sigma_{2s}=0.0306\pm0.0010$ Mb and $\sigma_{2p}=0.0704\pm0.0010$ Mb, so that $\sigma_2=0.1010$ Mb, versus the present LG (VG) values $\sigma_{2s}=0.0332$ (0.0335) Mb, $\sigma_{2p}=0.0922$ (0.0944) Mb, and $\sigma_2=0.1254$ (0.1279) Mb. It may be observed, however, that according to Fig. 3 of their work, $\sigma_2\approx0.12$ Mb, which is in better agreement with the present results. Thus it appears that the data of their Table I do not sum to the measured cross section, but rather to a Shore profile which reproduces poorly the maximum. The experimental ratio σ_{2p}/σ_{2s}, however, is about 2.3 against the present value 2.8. Their data at 71.3 eV, being close to an autoionizing state poorly resolved in their experiment, cannot be safely compared with the present results.

There is also some experimental evidence[11,14] that at the 1_3 resonance the minimum of σ_{2p} should occur at an energy slightly lower than that of σ_{2s}; the present calculations place these minima at 69.81 and 69.84 eV, respectively. The σ_2 results of Lindle *et al.*[11,14] (statistical error 2%, systematic error 10–15 %) agree rather well with the present ones in the range 69–71 eV. At the lower energies 67.9, 68.4, and 68.9 eV, these authors report 0.087, 0.094, and 0.087 Mb, versus the present LG (VG) values 0.105 (0.104), 0.103 (0.102), and 0.098 (0.097) Mb, not always within the stated experimental error. The present cross section is in very good agreement with the theoretical results of Salomonson *et al.*,[36] while the experimental data of Woodruff and Samson[8] lie rather lower between 70.1 and 71 eV (see Fig. 2 of Hayes and Scott[35]). Note that these last data are not normalized upon the West and Marr[4] value at 68.88 eV.

Figure 11 reports the calculated asymmetry parameter β_2 for the electrons leaving the ion in the $N=2$ level, together with the experimental results of Lindle *et al.*[11] The agreement with these is good and significantly better than those of Burkov *et al.*[34] and of Salomonson *et al.*[36] (see Fig. 14 of this last work). Since the present cross sections are in excellent agreement with those of these last authors, this implies that our phase shifts must be sensibly different from theirs. A few other measurements of β_2 are reported in the literature: Heimann *et al.*[12] found $\beta_2\approx-0.1$ at 66 eV and $\beta_2\approx0$ at 66.5 eV, while Schmidt *et al.*[9] found $\beta_2=0.01\pm0.09$ at 67.4 eV. The present results at these energies are, in the LG (VG), -0.107 (-0.092), -0.064 (-0.055), and 0.016 (0.024). Jiménez-Mier *et al.*[13] measured the angular dependence of the 304-Å fluorescence, a quantity which allows one to extract the ratio $\sigma_{2p\epsilon d}/\sigma_{2p}$. This ratio was found to be 0.25 ± 0.04 and 0.25 ± 0.03 at 65.5 and 66.5 eV, respectively, in good agreement with the present results of 0.28 at both energies and in both gauges.

Very recently, Zubek *et al.*[16] have measured the $N=2$ differential cross section at 0° with linearly polarized light. But for an energy shift, which lies inside their stated error ±15 meV in the energy calibration, the deep minima of the cross section in their Fig. 1 are reproduced accurately by the present calculations. Between 70 and 71 eV, however, a slower decrease is predicted, while the calculations of Hayes and Scott[35] find a faster one. It must be noted that the computation of this quantity is very delicate, since in this energy region the cross section and the asymmetry parameter are varying rapidly and in opposite directions.

A more important difference is found in the region of the -1_3 resonance, where the interpolated cross section of Zubek *et al.*[16] presents a dip which is not reproduced by the present calculations or by those of Hayes and Scott.[35] In our opinion, this feature may be an artifact of their interpolation formula, which contains intrinsically

such a dip. Moreover, the feature associated by these authors to the -1_3 resonance appears to lie amidst the positions predicted by the present calculations for the 2_4 and -1_3 resonances. It might be that these authors have seen the unresolved couple. This interpretation is also supported by the following facts: (i) the present width 0.037 eV agrees well with the other accurate theoretical values 0.039 eV (Refs. 26 and 30) and 0.030 eV,[25] (ii) the observed width 0.073 ± 0.015 eV is comparable with the calculated distance 0.092 eV between the 2_4 and -1_3 resonances, and (iii) the experiment was performed with a bandwidth of 0.050 eV.

IV. CONCLUSIONS

The results presented in this work show that, through the present procedure based on the K-matrix integral equation, energy-variational methods with L^2 basis sets may be applied successfully to many-channel problems and are capable of describing with great accuracy the resonance structures. The present method may work accurately also in the presence of many open channels, e.g., for molecular systems, and may employ many electronic configurations to describe accurately the electron correlation, as we have also verified for the Li^- and Na^- systems.[57,58] Finally, it should be pointed out that the method, by increasing wisely the size of the basis set, may handle also the energy regions close to the thresholds.

APPENDIX

As stated above, the channel indexes α and γ refer to open PWC subspaces (1 to n) while β refers to arbitrary ones (0 to N). The normalization properties of the states $|\Psi_{\alpha E}\rangle$, Eq. (4), may be determined as follows. By Eq. (1)

$$\langle\Psi_{\alpha'E'}|\Psi_{\alpha E}\rangle=S_{\alpha'E',\alpha E}+\sum_{\beta'}\oint d\epsilon'\mathrm{P}\frac{1}{E'-\epsilon'}K^*_{\beta'\epsilon',\alpha'E'}S_{\beta'\epsilon',\alpha E}+\sum_{\beta}\oint d\epsilon\mathrm{P}\frac{1}{E-\epsilon}K_{\beta\epsilon,\alpha E}S_{\alpha'E',\beta\epsilon}$$
$$+\sum_{\beta}\oint d\epsilon\sum_{\beta'}\sum d\epsilon' K^*_{\beta'\epsilon',\alpha'E'}\mathrm{P}\frac{1}{E'-\epsilon'}S_{\beta'\epsilon',\beta\epsilon}\mathrm{P}\frac{1}{E-\epsilon}K_{\beta\epsilon,\alpha E}$$

(the conjugate symbol, unnecessary in our case, is used for the generality of the proof) where $S_{\beta'E',\beta E}$ are the overlaps between the basis-set functions, which, due to the orthonormality inside each subspace, may be written in the form

$$S_{\beta'E',\beta E}=\delta_{\beta'\beta}\delta_{E'E}+(1-\delta_{\beta'\beta})S_{\beta'E',\beta E}$$

where $\delta_{E'E}$ is a Kronecker or Dirac δ for discrete and continuous states, respectively. Making use of this relation, one obtains

$$\langle\Psi_{\alpha'E'}|\Psi_{\alpha E}\rangle=\delta_{\alpha'\alpha}\delta(E'-E)+(1-\delta_{\alpha'\alpha})S_{\alpha'E',\alpha E}+\mathrm{P}\frac{1}{E'-E}K^*_{\alpha E,\alpha'E'}+\sum_{\beta'(\neq\alpha)}\oint d\epsilon'\mathrm{P}\frac{1}{E'-\epsilon'}K^*_{\beta'\epsilon',\alpha'E'}S_{\beta'\epsilon',\alpha E}$$
$$+\mathrm{P}\frac{1}{E-E'}K_{\alpha'E',\alpha E}+\sum_{\beta(\neq\alpha')}\oint d\epsilon\mathrm{P}\frac{1}{E-\epsilon}K_{\beta\epsilon,\alpha E}S_{\alpha'E',\beta\epsilon}+\sum_{\beta}\oint d\epsilon K^*_{\beta\epsilon,\alpha'E'}\mathrm{P}\frac{1}{E'-\epsilon}\mathrm{P}\frac{1}{E-\epsilon}K_{\beta\epsilon,\alpha E}$$
$$+\sum_{\beta}\oint d\epsilon\sum_{\beta'(\neq\beta)}\oint d\epsilon' K^*_{\beta'\epsilon',\alpha'E'}\mathrm{P}\frac{1}{E'-\epsilon'}S_{\beta'\epsilon',\beta\epsilon}\mathrm{P}\frac{1}{E-\epsilon}K_{\beta\epsilon,\alpha E}$$

and since[43]

$$\mathrm{P}\frac{1}{E'-\epsilon}\mathrm{P}\frac{1}{E-\epsilon}=\mathrm{P}\frac{1}{E'-E}\left[\mathrm{P}\frac{1}{E-\epsilon}-\mathrm{P}\frac{1}{E'-\epsilon}\right]+\pi^2\delta(E-E')\delta(E-\epsilon)$$

(of course, the last term survives the integration only for the open PWC's) one obtains

$$\langle\Psi_{\alpha'E'}|\Psi_{\alpha E}\rangle=\delta(E'-E)\left[\delta_{\alpha'\alpha}+\pi^2\sum_{\gamma}K^*_{\gamma E,\alpha'E}K_{\gamma E,\alpha E}\right]+(1-\delta_{\alpha'\alpha})S_{\alpha'E',\alpha E}+\mathrm{P}\frac{1}{E'-E}K^*_{\alpha E,\alpha'E'}$$
$$+\sum_{\beta'(\neq\alpha)}\oint d\epsilon'\mathrm{P}\frac{1}{E'-\epsilon'}K^*_{\beta'\epsilon',\alpha'E'}S_{\beta'\epsilon',\alpha E}+\mathrm{P}\frac{1}{E-E'}K_{\alpha'E',\alpha E}$$
$$+\sum_{\beta(\neq\alpha')}\oint d\epsilon\mathrm{P}\frac{1}{E-\epsilon}K_{\beta\epsilon,\alpha E}S_{\alpha'E',\beta\epsilon}+\mathrm{P}\frac{1}{E'-E}\sum_{\beta}\oint d\epsilon K^*_{\beta\epsilon,\alpha'E'}\mathrm{P}\frac{1}{E-\epsilon}K_{\beta\epsilon,\alpha E}$$
$$+\mathrm{P}\frac{1}{E-E'}\sum_{\beta'}\oint d\epsilon' K^*_{\beta'\epsilon',\alpha'E'}\mathrm{P}\frac{1}{E'-\epsilon'}K_{\beta'\epsilon',\alpha E}$$
$$+\sum_{\beta}\oint d\epsilon\sum_{\beta'(\neq\beta)}\oint d\epsilon' K^*_{\beta'\epsilon',\alpha'E'}\mathrm{P}\frac{1}{E'-\epsilon'}S_{\beta'\epsilon',\beta\epsilon}\mathrm{P}\frac{1}{E-\epsilon}K_{\beta\epsilon,\alpha E}\ .$$

All the terms but the first one cancel among themselves, as may be seen by substituting the expressions (3) for $K^*_{\alpha E,\alpha'E'}$, $K_{\alpha'E',\alpha E}$ $K^*_{\beta\epsilon,\alpha'E'}$, and $K_{\beta'\epsilon,'\alpha E}$.

*Electronic address: lencigh@icnucevm.cnuce.cnr.it.

[1]R. P. Madden and K. Codling, Astrophys. J. **141**, 364 (1965).
[2]W. S. Watson, J. Phys. B **5**, 2292 (1972).
[3]P. Dhez and D. L. Ederer, J. Phys. B **6**, L59 (1973).
[4]G. V. Marr and J. B. West, At. Data Nucl. Data Tables **18**, 497 (1976); J. B. West and G. V. Marr, Proc. R. Soc. London, Ser. A **349**, 397 (1976).
[5]P. R. Woodruff and J. A. R. Samson, Phys. Rev. Lett. **45**, 110 (1980).
[6]F. J. Wuilleumier, Ann. Phys. (Paris) **4**, 231 (1982).
[7]J. M. Bizau, F. Wuilleumier, P. Dhez, D. L. Ederer, T. N. Chang, S. Krummacher, and V. Schmidt, Phys. Rev. Lett. **48**, 588 (1982).
[8]P. R. Woodruff and J. A. R. Samson, Phys. Rev. A **25**, 848 (1982).
[9]V. Schmidt, H. Derenbach, and R. Malutzki, J. Phys. B **15**, L523 (1982).
[10]P. Morin, M. Y. Adam, I. Nenner, J. Delwiche, M. J. Hubin-Franskin, and P. Lablanquie, Nucl. Instrum. Methods **208**, 761 (1983).
[11]D. W. Lindle, T. A. Ferrett, U. Becker, P. H. Kobrin, C. M. Truesdale, H. G. Kerkhoff, and D. A. Shirley, Phys. Rev. A **31**, 714 (1985).
[12]P. A. Heimann, U. Becker, H. G. Kerkhoff, B. Langer, D. Szostak, R. Wehlitz, D. W. Lindle, T. A. Ferrett, and D. A. Shirley, Phys. Rev. A **34**, 3782 (1986).
[13]J. Jiménez-Mier, C. D. Caldwell, and D. L. Ederer, Phys. Rev. Lett. **57**, 2260 (1986).
[14]D. W. Lindle, T. A. Ferrett, P. A. Heimann, and D. A. Shirley, Phys. Rev. A **36**, 2112 (1987).
[15]H. Kossmann, B. Krässig, and V. Schmidt, J. Phys. B **21**, 1489 (1988).
[16]M. Zubek, G. C. King, P. M. Rutter, and F. H. Read, J. Phys. B **22**, 3411 (1989).
[17]R. S. Oberoi, J. Phys. B **5**, 1120 (1972).
[18]K. T. Chung, Phys. Rev. A **6**, 1809 (1972).
[19]V. L. Jacobs and P. G. Burke, J. Phys. B **5**, L67 (1972).
[20]D. R. Herrick and O. Sinanoglu, Phys. Rev. A **11**, 97 (1975).
[21]V. S. Senashenko and A. Wague', J. Phys. B **12**, L269 (1979).
[22]K. T. Chung and B. F. Davis, Phys. Rev. A **22**, 835 (1980).
[23]T. N. Chang, J. Phys. B **13**, L551 (1980).
[24]K. A. Berrington, P. G. Burke, W. C. Fon, and K. T. Taylor, J. Phys. B **15**, L603 (1980).
[25]S. Wakid and J. Callaway, Phys. Lett. **78A**, 137 (1980).
[26]Y. K. Ho, J. Phys. B **15**, L691 (1982).
[27]J. A. Richards and F. P. Larkins, J. Electron Spectrosc. Relat. Phenom. **32**, 193 (1983).
[28]P. C. Ojha, J. Phys. B **17**, 1807 (1984).
[29]P. Scott and P. G. Burke, J. Phys. B **17**, 1321 (1984).
[30]Y. K. Ho and J. Callaway, J. Phys. B **18**, 3481 (1985).
[31]S. Salomonson, S. L. Carter, and H. P. Kelly, J. Phys. B **18**, L149 (1985).
[32]C. D. Lin, Adv. At. Mol. Phys. **22**, 77 (1986); L. Lipsky, R. Anania, and M. J. Conneely, At. Data Nucl. Data Tables **20**, 127 (1977).
[33]C. A. Nicolaides and Y. Komninos, Phys. Rev. A **35**, 999 (1987).
[34]S. M. Burkov, N. A. Letyaev, S. I. Strakhova, and T. M. Zajac, J. Phys. B **21**, 1195 (1988).
[35]M. A. Hayes and M. P. Scott, J. Phys. B **21**, 1499 (1988).
[36]S. Salomonson, S. L. Carter, and H. P. Kelly, Phys. Rev. A **39**, 5111 (1989).
[37]I. Cacelli, R. Moccia, and V. Carravetta, in *Collisions and Half Collisions with Lasers,* edited by N. K. Rahman and C. Guidotti (Harwood, Chur, 1982), p. 229.
[38]I. Cacelli, R. Moccia, and V. Carravetta, Chem. Phys. **90**, 313 (1984).
[39]R. Moccia and P. Spizzo, J. Phys. B **18**, 3537 (1985); **18**, 3555 (1985).
[40]R. Moccia and P. Spizzo, J. Phys. B **20**, 1423 (1987).
[41]R. Moccia and P. Spizzo, J. Phys. B **21**, 1121 (1988); **21**, 1133 (1988); **21**, 1145 (1988).
[42]R. Moccia and P. Spizzo, Phys. Rev. A **39**, 3855 (1989).
[43]U. Fano, Phys. Rev. **124**, 1866 (1961); U. Fano and J. W. Cooper, Rev. Mod. Phys. **40**, 441 (1968).
[44]C. J. Joachain, *Quantum Collision Theory* (North-Holland, New York, 1975).
[45]A. F. Starace, in *Corpuscles and Radiation in Matter I,* Vol. 31 of *Encyclopedia of Physics,* edited by W. Mehlhorn (Springer-Verlag, Berlin, 1982), p. 1.
[46]P. G. Burke and W. D. Robb, Adv. At. Mol. Phys. **11**, 143 (1975).
[47]I. Cacelli, V. Carravetta, and R. Moccia, J. Chem. Phys. **85**, 7038 (1986).
[48]D. E. Freund, B. D. Huxtable, and J. D. Morgan III, Phys. Rev. A **29**, 980 (1984).
[49]D. P. Carroll, H. J. Silverstone, and R. M. Metzger, J. Chem. Phys. **71**, 4142 (1979).
[50]M. L. Goldberger and K. M. Watson, *Collision Theory* (Wiley, New York, 1967); J. R. Taylor, *Scattering Theory* (Wiley, New York, 1972); B. H. Brandsen, *Atomic Collision Theory* (Benjamin, New York, 1970).
[51]U. Fano and J. W. Cooper, Phys. Rev. **137**, A1364 (1965).
[52]M. E. Rose, *Elementary Theory of Angular Momentum* (Wiley, New York, 1957).
[53]E. R. Cohen and B. N. Taylor, Rev. Mod. Phys. **59**, 1121 (1987); J. Phys. Chem. Ref. Data **2**, 663 (1973).
[54]A. K. Bhatia and A. Temkin, Phys. Rev. A **11**, 2018 (1975).
[55]S. Bashkin and J. O. Stoner, *Atomic Energy Levels and Grotrian Diagrams I* (North-Holland, Amsterdam, 1975); the energy in cm^{-1} was converted by 1 eV = 8065.541 cm^{-1} (Ref. 53).
[56]B. W. Shore, Phys. Rev. **171**, 43 (1968).
[57]R. Moccia and P. Spizzo, J. Phys. B **23**, 3557 (1990).
[58]R. Moccia and P. Spizzo, Nuovo Cimento (to be published).